

# How do LLMs Support Deep Learning Testing? A Comprehensive Study Through the Lens of Image Mutation\*

Liwen Wang<sup>1,2,†</sup>, Yuanyuan Yuan<sup>2</sup>, Ao Sun<sup>2</sup>, Zongjie Li<sup>2</sup>, Pingchuan Ma<sup>2</sup>, Daoyuan Wu<sup>2</sup>, Shuai Wang<sup>2</sup>  
<sup>1</sup>*Xidian University*, <sup>2</sup>*The Hong Kong University of Science and Technology*  
 liwenwang@stu.xidian.edu.cn, {yyuanaq, asunac, zligo, pmaab, daoyuan, shuaiw}@cse.ust.hk

## Abstract

Visual deep learning (VDL) systems have demonstrated their capability to understand complex image semantics, paving the way for significant real-world applications like image recognition, object detection, and autonomous driving. To evaluate the reliability of VDL, a mainstream approach is software testing, which requires diverse and controllable mutations over image semantics. The rapid development of multi-modal large language models (MLLMs) has introduced revolutionary image mutation potentials through instruction-driven methods. Users can now freely describe desired mutations and let MLLMs generate the mutated images. Hence, parallel to large language models’ (LLMs) recent success in traditional software fuzzing, one may also expect MLLMs to be promising for VDL testing in terms of offering diverse and complex image mutations.

However, the quality of MLLM-produced test inputs in VDL testing remains largely unexplored. We present the first study, aiming to assess MLLMs’ adequacy from 1) the semantic *validity* of MLLM mutated images, 2) the *alignment* of MLLM mutated images with their text instructions (prompts), 3) the *faithfulness* of how different mutations preserve semantics that are ought to remain unchanged, and 4) the *effectiveness* of detecting VDL faults. With large-scale human studies and quantitative evaluations, we identify MLLM’s promising potentials in expanding the covered semantics of image mutations. Notably, while SoTA MLLMs (e.g., GPT-4V) fail to support or perform worse in editing existing semantics in images (as in traditional mutations like rotation), they generate high-quality test inputs using “semantic-additive” mutations (e.g., “dress a dog with clothes”), which bring extra semantics to images; these were infeasible for past approaches. Hence, we view MLLM-based mutations as a vital *complement* to traditional mutations, and advocate future VDL testing tasks to combine MLLM-based methods and traditional image mutations for comprehensive and reliable testing.

\*Corresponding Authors: Yuanyuan Yuan (yyuanaq@cse.ust.hk) and Shuai Wang (shuaiw@cse.ust.hk)

<sup>†</sup>This work was done when Liwen Wang was interning at HKUST.

## 1 Introduction

Visual deep learning (VDL) systems comprehend semantics of image contents to enable a wide range of real-world applications (e.g., autonomous driving, medical imaging diagnosis) that were previously human-reliant. However, since the decision rules of VDL are obscure, such as how a VDL system recognizes cars, VDL systems can experience drastic failures in their outputs, which jeopardizes the reliability of VDL systems in safety-critical applications. Software testing has been very effective in detecting VDL failures; it mutates input images and defines testing oracles over varying mutation schemes (e.g., VDL outputs should be invariant to the rotation of the input). A VDL failure can be detected as a violation of the oracle. In recent years, our community has proposed a variety of mutation schemes for VDL testing under different scenarios, such as image classification [62], object detection [57], image captioning [64], and autonomous driving [46, 56, 67].

Inputs of VDL systems are images whose contents have rich semantics. Thus, to evaluate the reliability of VDL systems via software testing, comprehensively covering different image semantics is demanding for the input mutation. Nevertheless, mutating image semantics is fundamentally challenging because the relation between pixel values and most image semantics is unclear and hard to model [27, 37, 42, 52, 65, 72]. Existing methods operating on pixels can only mutate some basic semantics such as brightness and contrast [46]. Also, the mutation must be controllable; an arbitrary mutation itself can violate the testing oracle and induce an invalid testing input. Previous works achieve controllable mutations for more complex semantics using representation learning techniques [52, 67, 71], which require image samples containing the expected mutations and are limited to certain VDL inputs such as driving scenes [67] or face photos [52].

The recent multi-modal large language models (MLLMs)<sup>1</sup> (e.g., GPT-4V [5]) have liberated the freedom of diverse and

<sup>1</sup>Since MLLMs are often jointly used with other large models such as Diffusion model [30], CLIP [48], DALLÉ [3], etc., to minimize confusion, we use MLLMs as a general term for them. We use their own names when referring to their special usage.

controllable mutations for image semantics: users can freely describe the anticipated mutation in natural language and let MLLMs generate the mutated images. This smooth translation between text descriptions and images is shedding light on a new paradigm of image mutation, namely *instruction-driven mutation*, that supports various traditional mutations (see the introduction in Sec. 3) in a unified prompt-driven manner, and also offers a wide range of new mutations that are hardly achievable by traditional methods. Thus, one may reasonably anticipate that MLLMs can revolutionize VDL testing, in parallel to large language model (LLM)’s emerging adoption and success in our community to boost traditional software testing [15, 55, 60], program repairing [20, 47, 61], and program synthesis [6, 34, 59].

Despite the optimism towards MLLM-empowered VDL testing, the internals of MLLMs (i.e., how they generate outputs) are hard to interpret. Unlike traditional mutations that form constraints (e.g., explicit mathematical formulas; see Sec. 3.1) to control the mutated semantics, MLLMs lack guarantees on whether the mutations are achieved as expected. Notably, due to the underlying deep learning techniques, modern VDL systems do not have effective input checkers. Thus, a semantically *invalid* image can be accepted by a VDL system to produce a *valid* (but incorrect) output. Some recent reports have shown that MLLMs can generate semantically invalid images [10, 18, 21], which makes the follow-up testing and the detected VDL failures meaningless (as those failures can hardly occur in real-world scenarios). Thus, it is demanding to systematically evaluate MLLM’s capability in mutating VDL test inputs.

This paper first presents a taxonomy on image semantics at different granularities and reviews how they are covered by traditional mutation methods and the instruction-driven mutation of MLLMs. Then, for each category of semantics, we assess the quality of test inputs generated by traditional mutations and MLLMs. Following common practice in VDL testing [56, 62, 67], quality is measured from 1) the *validity* of semantics in mutated images, 2) the *alignment* of mutated images with text instructions, 3) the *faithfulness* of how different mutations preserve semantics that should be unchanged, and 4) the *effectiveness* of detecting VDL faults.

We consider ten representative types of mutations and four recent SoTA MLLMs including GPT-4V. Our evaluated datasets cover general image classification [14], fine-grained dog breed identification [2], face recognition [36], and autonomous driving [13]. We conduct large-scale human studies through Amazon Mechanical Turk [1] by hiring 20 Ph.D. students experienced in VDL systems and software testing. They evaluate 2,300 image mutations, and each mutation is rated by two human participants w.r.t. our criteria. We also conduct quantitative evaluations to measure the quality of test inputs. Our results reveal that MLLM-enabled mutations and traditional mutations are complementary in VDL testing: MLLMs cannot replace traditional mutation methods but bring a new

dimension to image mutations. Specifically, while MLLMs can alternatively implement traditional mutations with proper text prompts, the re-implemented mutations exhibit low faithfulness and alignment. For example, none of our evaluated SoTA MLLMs can achieve image rotation. On the other hand, although MLLMs cannot edit existing semantics in images as well as traditional mutations, they perform impressively well on “semantic-additive” mutations that add new semantics to the seed images (e.g., “*adding glasses for a dog in an image*”), which are uniquely enabled by MLLMs. In sum, this paper makes the following key contributions:

- This paper conducts the first study on the quality of test inputs generated by MLLM for VDL testing. It also studies the role and positioning of MLLM’s instruction-driven mutation w.r.t. traditional mutation paradigms.
- We present a systematic review of existing image mutations in VDL testing. We also design large-scale human studies and quantitative evaluations to assess the quality of test inputs from the validity, alignment, faithfulness, and effectiveness perspectives.
- Our findings better position MLLMs and their enabled instruction-driven mutations in VDL testing. While MLLMs cannot well edit existing semantics in images like traditional mutations, they enable adding new semantics, thus expanding VDL testing’s scope.

## 2 Background: VDL Testing

Holistically speaking, a VDL system typically consists of a visual understanding module and a decision module. The visual understanding module takes an image as input and extracts features from its content. The decision module yields outputs (according to the specific VDL application domain) based on the extracted features. From this perspective, image classifier, object detector, image captioner, and auto-driving systems, etc., that were widely tested in our community can all be counted as VDL systems [46, 56, 57, 62, 64].

The vanilla way of evaluating VDL systems is comparing their outputs with human annotations over a set of test inputs (i.e., labeled images in standard test datasets). However, manually annotating test inputs is labor-intensive, impeding automated and large-scale evaluations. Software testing has achieved remarkable success in evaluating the reliability of VDL systems. It uses different input mutation schemes to generate diverse test inputs and forms oracles to enable automatic “annotations” for the test inputs. For example, a rescaled image should have the same output as the original image when fed into an object detector. This way, software testing can identify VDL faults as violations of testing oracles, where human annotations are no longer required.

**Test Input Generation.** Given that VDL processes semantics of image contents, existing works have proposed various mutations to modify image semantics; we elaborate on them in

Sec. 3. Note that different from adversarial perturbations<sup>2</sup> that add noise to images or change a few pixels, semantic-level mutations in VDL testing holistically alter images to diversify image semantics, exploring different usage scenarios of VDL systems.

**Testing Oracle.** Metamorphic testing (MT) stands as one mainstream testing paradigm of VDL testing in recent years [56, 57, 62, 64–67]. MT checks whether a VDL system’s outputs are aligned with the relation defined in an MT testing oracle, when the VDL is processing an input and its mutated version. Unalignment shows that one of the inputs is ill-processed. Since testing oracles are critical to detect VDL faults, input mutations cannot be arbitrary and should properly preserve the oracle; see examples in Sec. 3.

### 3 Image Mutations

**Image Decomposition: A Motivating Example.** To understand how VDL works and how existing input mutations are designed, we first decompose the dog image in Fig. 1 into different semantics. Starting from a lower level, the image can be seen as a matrix of pixels, and the magnitude of pixel values determines the brightness and contrast of the image. Besides, the spatial arrangement of pixels reflects geometrical properties of the image, such as the scale and the rotation angle. A reliable VDL system that recognizes dogs should be resilient to changes of these semantics. At a higher level, the image contains a dog and the background grass; the dog itself has rich semantics such as the action and the orientation. Similarly, the semantics in background may vary with the working scenario of the VDL, e.g., the grass may be replaced by snow in a winter scene. Overall, the dog-recognition VDL should focus on the semantics of the dog and be invariant to irrelevant semantics in the background.

Based on the above semantic decomposition, the following image mutation schemes have been proposed by existing works.

#### 3.1 Explicit & Mathematical Transformations

**Pixel-level.** Image brightness and contrast can be mutated by uniformly changing pixel values. In general, mutations belonging to this category can be formed as  $\mathbf{x} \text{ op } c$ , where  $c$  is a scalar value and  $\mathbf{x}$  is a matrix denoting the seed image.  $\text{op}$  decides the mutated semantics. For example,  $\text{op}$  is the add operation if the mutation changes the image brightness, that is, to increase the brightness of  $\mathbf{x}$ , all pixel values in  $\mathbf{x}$  can be increased by  $c$ . Similarly, mutating image contrast can be formulated as  $\mathbf{x} \times c$ , which enlarges the difference between pixel values in  $\mathbf{x}$ . Examples are in Fig. 1.

**Geometrical-level.** As geometrical properties are determined by the spatial arrangement of pixels, existing works implement these mutations using affine transformations, which essentially move pixels to new localizations and preserve the

image’s parallelism (i.e., two parallel lines remain parallel in the mutated image). Formally, suppose pixels of the image  $\mathbf{x}$  locate in a rectangular coordinate and the centering pixel is the original, the  $(i, j)$ -th pixel’s localization in the mutated image can be calculated as  $[i', j']^T = \mathbf{A} \times [i, j]^T + \mathbf{b}$ , where  $\mathbf{A}$  and  $\mathbf{b}$  characterize the geometrical mutation. For example, the values of  $(\mathbf{A}, \mathbf{b})$  of scaling and translation mutations are shown as  $(\mathbf{A}_S, \mathbf{b}_S)$  and  $(\mathbf{A}_T, \mathbf{b}_T)$  in Eq. 1, respectively,

$$\mathbf{A}_R = \begin{bmatrix} \cos(\theta) & -\sin(\theta) \\ \sin(\theta) & \cos(\theta) \end{bmatrix}, \mathbf{b}_R = \mathbf{0}; \mathbf{A}_T = \mathbf{0}, \mathbf{b}_T = \begin{bmatrix} t_x \\ t_y \end{bmatrix} \quad (1)$$

where  $\theta$  specifies the rotating angle.  $t_x$  and  $t_y$  indicate the vertical and horizontal translation distances. See examples in Fig. 1.

The aforementioned mutations are preferred in early VDL testing works due to their neat and explicit formulations [46, 56, 62]. These mutations are controllable and faithfully preserve semantics that shouldn’t be changed. The generated images are always valid (if the mutation is not iteratively applied). However, such explicit-formed mutations require knowing the precise relation between semantics and each pixel. Currently, only a few mutations are explicit-formed, largely limiting the diversity of covered image semantics.

#### 3.2 Implicit & Data Exploration

Some recent researches diversify the mutated semantics with data-driven mutations. These mutations implicitly explore patterns in a set of images and then apply the patterns to mutate a seed image.

**Style-level.** From a high level, each image can be decomposed as its style and content, and VDL systems should primarily focus on the content rather than style. Thus, existing VDL testing works propose different style-level mutations, whose generated images have distinct styles but presumably retain the content of the seed image. The “style” has been studied from two aspects. First, the style can be viewed as describing how the image is produced, e.g., the seed image in Fig. 1 is taken in reality and its style is “natural”. In that sense, the style can be changed by generating an image’s artistic-stylized variants (e.g., an image having the same dog but painted using a Van Gogh style, as in Fig. 1) [65]. Also, some works decompose a weather condition as the style and separate it from the main content. The weather conditions are transferred between images to generate test inputs; see Fig. 1. These weather-related mutations are often used to test VDL-based autonomous driving [67].

Existing style-level mutations are implemented using generative adversarial nets (GANs) and their success highly relies on the cycle-consistency [74]: decomposing and transferring styles are only applicable to images of similar content [73]; see results in Sec. 6.2.

**Perceptual-level.** The latest VDL testing has been focusing on fine-grained semantics of the objective in images, e.g., as shown in Fig. 1, the dog’s eyes and mouth can be mutated

<sup>2</sup>Such perturbations are leveraged by adversarial attacks to generate malicious inputs (i.e., adversarial examples) to fool a VDL system [25].

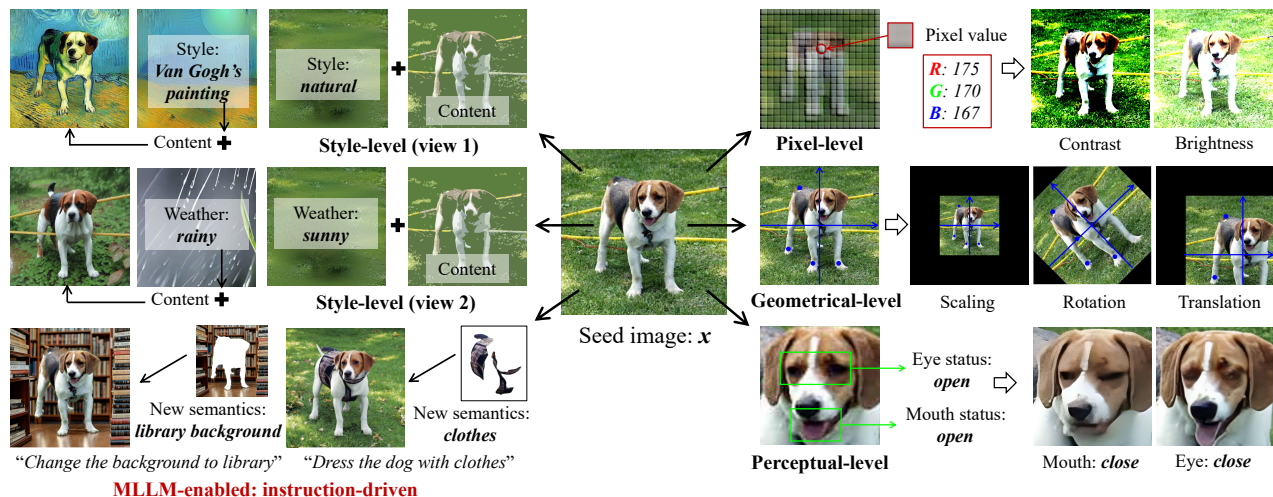


Figure 1: Decomposition of image semantics and their corresponding mutation schemes.

to evaluate whether the VDL accurately recognizes different dogs. Such mutations are often known as perceptual-level mutations [65] and aim to edit the status of existing semantics in images [19, 65]. Perceptual-level mutations employ generative models (e.g., GANs [36]) to obtain a semantic-level *latent* representation for each image. Instead of operating on the pixel values (as in mutations mentioned in Sec. 3.1), they manipulate the latent representation to achieve the mutation.

To control the mutation and generate valid test inputs, perceptual-level mutations rely on a hypothesis: when projected into the latent space using a well-developed generative model, semantically meaningful images concentrate as clusters and each cluster corresponds to images of similar semantics [40, 65]. For instance, if two clusters  $a$  and  $b$  in the latent space contain left- and right-oriented dogs, respectively, slightly moving an image’s latent coordinate towards the direction  $a \rightsquigarrow b$  can mutate the dog’s orientation in the image generated using this new latent coordinate [52]. We refer interested readers to [52, 71] for details of perceptual-level mutations.

### 3.3 MLLM-Based Mutations

In line with past image mutations in VDL testing, we explain how MLLMs can boost the mutation schemes from two aspects.

**Instruction-Driven.** MLLM’s success in the multimodal domain has revolutionized the image mutation paradigm. MLLMs enable translation between text and images, such that users can freely describe their anticipated mutation to a seed image using text instruction; MLLMs then generate the mutated image according to the instruction. This instruction-driven paradigm largely expands the covered semantics in image mutations and liberates the users’ freedom to design the anticipated mutations. Moreover, by designing the proper

text instruction, previous mutations discussed in Sec. 3.1 and Sec. 3.2 can be uniformly implemented using MLLMs.

**Semantic-Additive.** Besides the unified implementation of mutations mentioned above, the instruction-driven paradigm also introduces a new category of mutations, which we refer to as semantic-additive mutations. Instead of modifying existing semantics in images, these mutations can bring new semantics to the seed image (which are nearly infeasible using previous mutations). For example, the dog image in Fig. 1 can be decorated with clothes to challenge the VDL system under test. Essentially, such additive capability enables a new dimension for the input mutation in VDL testing.

Knowledgeable readers may wonder the differences between semantic-additive mutations with the object insertion adopted in testing object-based VDL systems [57, 64, 66]. We clarify that semantic-additive mutations operate in semantic-level and are finer-grained, which often require reasoning the relation and hierarchy between semantics (either intra- or inter-object). For example, the “dressing with clothes” mutation in Fig. 1 needs to understand and identify the dog’s body and *replace* it with appropriate clothes. Object insertion, in contrast, does not perceive image semantics and only relies on object locations in the image, so that the inserted object will not overlap with existing ones. Since object insertion mostly applies to object-based VDL systems (e.g., the inserted object may affect the classification result), we omit it in this study.

## 4 Research Motivations

**Limitations of Past Methods.** Though the fast development of input mutations in VDL testing has achieved fine-grained control over higher-level image semantics, they only apply to limited scenarios and specific seeds. Noteworthy, existing perceptual-level mutations (the most recent and effective mutation) require humans to annotate the mutated semantics in each seed and let humans validate and interpret the achieved

mutation [52, 71]; this process only applies to highly aligned images (e.g., face photos taken in a front view where a unified mask can be adopted to pinpoint eyes, mouth, etc.) and can hardly be automated in practice. From this perspective, it is expected that MLLMs can offer a more general, automated, and highly flexible mutation scheme for VDL testing. The mutations can be controlled by text instructions, which are more intuitive, accessible, and calibratable to users than past methods.

**Unclear MLLM Internals.** Despite the optimism, the internals of how such mutations are achieved by MLLMs remain unclear. Previous explicit mutations (pixel- and geometrical-level mutations mentioned in Sec. 3.1) are rigorously implemented according to their mathematical definitions. Implicit mutations (style- and perceptual-level mutations in Sec. 3.2) often rely on well-developed generative models to ensure generating valid images; the usefulness of these methods has been empirically justified in recent works [16, 35, 65].

In contrast, per recent reports, MLLMs often fail to mutate images according to the given instructions [41], and may generate broken and ill-formed images from time to time [10, 18, 21]. Hence, we believe our community still lacks understanding of how exactly MLLMs can boost VDL testing, and a comprehensive study is urgent for VDL developers to understand MLLM’s (in-)capability of mutating images, especially in the context of VDL testing where the quality of mutated test inputs is crucial.

## 5 Research Study Setup

Our key research question (RQ) is on MLLM’s capability of generating test inputs for VDL testing. To this end, we conduct both human studies and quantitative evaluations to assess if MLLM can support varying mutations noted in Sec. 3. The setups are introduced below.

### 5.1 Evaluated Aspects

Following Sec. 4, we focus on four aspects to assess the quality of image mutations (both traditional and MLLM-enabled) for VDL testing. These four aspects include three input-side requirements, and one output-side assessment.

**Alignment.** The achieved mutation must be aligned to the expectation. This is important as users need to know which mutated semantics trigger VDL faults and diagnose the VDL’s faulty behavior using the testing results. For example, if a rotation mutation does not rotate the image as expected, users will falsely interpret the tested VDL system as behaving correctly (*false negatives*).

**Faithfulness.** A mutation should faithfully preserve the semantics that are ought to be unchanged. For example, to close eyes of face photos, the mutation should let other semantics (e.g., background, hair, nose) remain unchanged and only close the eyes. Otherwise, the unanticipated mutation may break the testing oracle and brings *false positives*. The follow-up diagnosis for VDL’s faulty behaviors can also be misled.

**Validity.** Different from traditional software (e.g., a sorting algorithm) that implement input checker like type checker, the deep learning module in modern VDL system often does not support checking whether an input image is semantically valid. Since input images are represented as numerical matrices, the VDL system can evoke all computations and generate a valid, but random output when taking an image containing only noise or a fragmented image.

Overall, from a high level, alignment focuses on the mutated semantics whereas faithfulness asserts the unchanged semantics. Validity more holistically assesses the semantics in the whole image.

**Testing Effectiveness.** Further to the above three input-side requirements, we also consider the testing effectiveness as an output-side assessment: we check how well the mutated images can detect VDL faults. This is crucial as we need to assess whether a mutation is valuable. The MLLM’s instruction-driven paradigm is free-form, meaning that innumerable mutations can be (potentially) enabled. For effective and efficient testing, users require assessing which mutations are more useful in detecting VDL faults.

### 5.2 MLLMs and Their Pipelines

We evaluate four SoTA and representative MLLMs that support both text and image inputs, including LLaVA [43], CogVLM [58], GPT-4V [5], and InstP2P [8].

**Dialog-Based.** The most straightforward way to mutate images is establishing a dialog with the MLLM, as shown in Fig. 2(a). For example, the users first provide the seed image and a prompt of the mutation instruction to GPT-4V and let GPT-4V return the mutated image. However, our preliminary explorations show that this dialog-based pipeline fails to generate test inputs in *all* cases we try: GPT-4V either generates an entirely new image (nearly all semantics are changed) or fails to achieve the mutation (i.e., GPT-4V responds that it cannot generate the image).

To alleviate this issue, one may expect using prompt engineering to better guide the MLLM. Nevertheless, our preliminary study shows that it is hard to tune MLLM prompts and achieve constantly improved performance. Moreover, we argue that “tuning prompts” is less practical in our context, as VDL developers (main users of VDL testing tools) are often not experts in prompt engineering; MLLM should provide out-of-the-box support for implementing mutations. Therefore, following suggestions in [9, 11, 22, 32, 33], we consider optimizations over the mutation pipeline and equip the MLLM with Diffusion model [4], a more sophisticated image generation model, as introduced below.

**Unidirectional & Fine-tuning-based.** InstP2P designs an unidirectional pipeline (Fig. 2(b)) which directly uses a text instruction (the MLLM is employed to extract text features) and the seed image to generate the mutated image. In general, since the text instruction primarily describes the mutation and does not include details in the images, InstP2P fine-tunes the

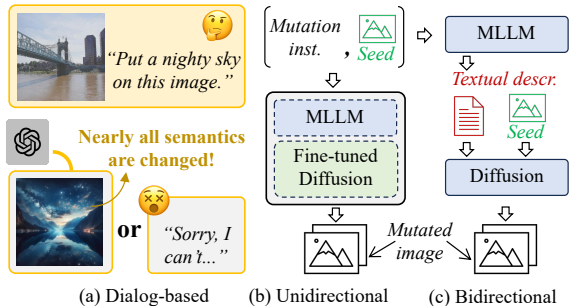


Figure 2: Pipelines of MLLM-based mutations.

pre-trained Diffusion model for a diverse set of mutations. Each fine-tuning data point consists of a seed image and its mutated variant, and the Diffusion model is trained to generate the mutated image when given the seed image and the corresponding text instruction. We refer interested readers to [8] for the fine-tuning details.

**Bidirectional & Post-hoc.** Another pipeline, as designed in [9, 11, 22, 32, 33], leverages MLLMs to transform the mutation instruction based on the seed image, such that details in the seed image can be included in the transformed instruction. This pipeline is categorized as bidirectional (Fig. 2(c)) as it implements the workflow of image  $\rightarrow$  text  $\rightarrow$  image. Specifically, due to MLLM’s promising capability of understanding images, users first feed the seed image to the MLLM and let the MLLM describe what the image would look after applying a mutation. Here, the MLLM’s output is a textual description of semantic-level details in the mutated image. This finer-grained text description, together with the seed image, are then fed to the Diffusion model to generate the mutated image. The superiority of this pipeline (compared with the dialog-based one) has been empirically justified in [11, 22, 32, 33].

Overall, the bidirectional pipeline, to some extent, achieves an automated prompt engineering by enriching the mutation instruction with the seed image’s details. The unidirectional pipeline, on the other hand, fine-tuning the Diffusion model to strengthen its capability in achieving image mutations. In our evaluations, we implement CogVLM, LLaVA, and GPT-4V with the bidirectional pipeline, and use the original unidirectional pipeline for InstP2P.

### 5.3 Datasets and Mutations

Table 1 lists the evaluated datasets. They are large-scale and representative to cover different application scenarios. ImageNet consists of 1,000 classes of real-life images, and is widely used for general image classification tasks. Dog-Breed dataset contains dog images with 120 different breeds and is a subset of ImageNet. It is constructed to improve VDL model’s accuracy in domain-specific applications. FFHQ includes human face photos; it is widely used for face recognition and annotation tasks. CityScape is composed of urban street scene

images, which are popular in autonomous driving, object detection, and instance segmentation, etc.

Table 1: Evaluated datasets.

Dataset	#Classes	Description	VDL Tasks
ImageNet [14]	1,000	Diverse real-life images	Image Classification
Dog-Breed [2]	120	Dog images of diff. breeds	Image Classification
FFHQ [36]	N/A	Human face photos	Face recognition, annotation, etc.
CityScape [13]	N/A	Urban street scene images	Autonomous driving, object detection, instance segmentation, etc.

Table 2: Evaluated mutations and their text instructions when implemented with MLLMs.

Mutation	Type	Instruction
① Contrast	Pixel	“Increase the contrast of the image.”
② Rotation	Geometrical	“Rotate the image 180 degrees.”
③ Artifying	Style	“Change the style of this image to Van Gogh style.”
④ Snow <sub>G</sub>		“What would it look like if it were snowing.”
⑤ Snow <sub>D</sub>		“What would it look like if it were snowing.”
⑥ Eyes	Perceptual	“Make the eyes of the person close.”
⑦ Background	Semantic-additive	“Change the background to a library.”
⑧ Clothes		“Dress the dog with clothes.”
⑨ Legs		“Change the dog’s legs to be bionic.”
⑩ Glasses		“Put on a pair of glasses for the dog.”

Aligned to different types of mutations introduced in Sec. 3, we consider six mutations (covering all four types) supported by traditional methods, as shown in Table 2. Specifically, since the weather transfer mutation is affected by the to-be-mutated image, we evaluate it on both general images (Snow<sub>G</sub> in Table 2) and driving scene photos (Snow<sub>D</sub> in Table 2) from ImageNet and CityScape, respectively. The perceptual-level mutation is achieved using GANs [71] and is dataset-specific, which only applies to aligned face photos in FFHQ. We also consider four different semantic-additive mutations that are uniquely enabled by MLLM. They operate in different granularities and manifest varying characteristics, as implied in the last column of Table 2. Considering that ⑧-⑩ require specifying the mutated object in the image, to evaluate them uniformly on diverse images, we use the Dog-Breed dataset.

To implement a mutation (either traditional or MLLM-enabled) using MLLMs, a text instruction (i.e., prompt) is required. We list the text instruction of each mutation in Table 2. Recall as mentioned in Sec. 5.2, we consider two optimized MLLM pipelines that are specifically designed for achieving image mutations, so that a mutation’s prompt can be a single-sentence instruction, enabling out-of-the-box usage. Due to such a simple form, we find that the MLLM is mostly robust to changes over those instructions, and we observe that, the instruction’s wording, grammatical structure, etc., does not notably impact the achieved mutation.

## 6 Human Studies

We form a group of 20 participants to evaluate the ten mutations in Table 2 according to the alignment, faithfulness, and

Table 3: Results of human evaluations. We mark results within  $[0, 1)$ ,  $(2, 4]$ , and  $(4, 5]$  in red, blue, and green, respectively.

Metric		Contrast	Rotation	Artifying	Snow <sub>G</sub>	Snow <sub>D</sub>	Eyes	Background	Clothes	Legs	Glasses
Alignment	LLaVA	0.8	0.0	3.2	2.3	4.3	1.3	1.3	1.9	1.8	3.8
	CogVLM	0.6	0.1	3.1	2.0	3.3	0.7	1.1	1.4	1.3	2.4
	GPT-4V	0.7	0.1	3.1	2.1	3.8	1.8	1.3	2.3	2.1	3.2
	InstP2P	1.2	0.0	2.5	0.6	0.1	0.1	2.6	0.7	1.1	4.2
	Traditional	4.9	4.9	1.7	0.1	4.2	4.1	N/A	N/A	N/A	N/A
Faithfulness	LLaVA	3.0	3.6	3.3	2.5	2.0	3.3	2.9	3.0	3.0	3.5
	CogVLM	2.7	3.5	3.0	2.3	2.0	3.0	2.8	2.5	3.1	3.3
	GPT-4V	3.0	3.7	3.3	2.7	2.1	3.0	3.0	2.8	3.1	3.5
	InstP2P	4.9	1.0	4.2	4.6	5.0	3.3	3.0	4.2	4.5	4.3
	Traditional	5.0	4.9	4.6	4.5	0.2	4.4	N/A	N/A	N/A	N/A
Validity	LLaVA	4.0	4.5	4.1	4.0	2.8	3.1	3.1	3.3	3.6	4.4
	CogVLM	3.6	4.3	3.7	3.8	2.7	2.5	2.9	3.2	3.6	4.0
	GPT-4V	4.0	4.2	3.9	3.8	2.9	2.5	3.1	3.3	3.8	4.5
	InstP2P	4.9	0.9	4.1	4.8	4.9	3.6	2.6	4.2	4.5	4.2
	Traditional	5.0	4.9	4.4	4.5	2.5	4.4	N/A	N/A	N/A	N/A

Green : Perfectly satisfy. Blue : Satisfy. Red : Fail.

validity requirements (discussed in Sec. 5.1). The effectiveness of these mutations in triggering VDL faults is evaluated using quantitative evaluations in Sec. 7.3. Since evaluating if a mutation fulfills these requirements needs inspecting how the changed semantics (both anticipated and unanticipated) may affect the downstream VDL testing and analysis, we hire 20 Ph.D. students experienced in software testing and VDL system in our human study.

## 6.1 Human Study Design

For each mutation listed in Table 2, we prepare 50 seed images to mutate. That is, for the six traditional mutations, each of them has  $50 \times 5 = 250$  mutated images, and for the four MLLM-enabled mutations, each of them has  $50 \times 4 = 200$  mutated images.

The common practice, as in most existing MLLM works [53, 68], is letting humans rank different mutated images. However, we observed that MLLMs can fail in implementing a mutation or generating valid images, which cannot be reflected from the ranking results. To address this, we design the questions as follows. Each question in our human study is formed by a seed image and one of its mutated variants (using different implementations), and a participant is asked to give a score (0 to 5) for the *alignment*, *faithfulness*, and *validity* of a mutated image. A zero score indicates that the mutated image fails to satisfy one requirement. For example, if the rotation mutation implemented using a MLLM does not rotate an image, the alignment score should be zero. We use scores 1-5 to assess each requirement because one mutation has maximal five different implementations (i.e., one traditional method + four MLLMs); the five different choices can distinguish different implementations.

We let each participant evaluate one of the ten mutations, in the sense that interchangeably evaluating different mutations

may confuse the participants, especially for subtle mutations that require careful comparison. Therefore, each participant answers 200 (for MLLM-enabled mutations) or 250 (for traditional mutations) questions. To reduce personal preferences of participants, each mutation is assigned to two different participants. The orders of the questions are shuffled to avoid potential bias due to question orders.

Before starting the human study, we prepare a 30-minute teaching for each participant. The teaching primarily aims to introduce the three requirements (i.e., alignment, faithfulness, and validity) with different successful and failed examples. It also gives participants suggestions on giving scores. For instance, zero indicates an unsatisfied requirement, and the scores should be distinguishable. Our human study is conducted using the Amazon Mechanical Turk platform [1]. We do not set time limit for each question because we expect participants to carefully assess the mutated images. The participant can pause and resume the evaluation at any time to avoid fatigue. The average time to finish all evaluation questions (i.e., 200 or 250) is around two hours as reported by participants.

## 6.2 Human Study Results

Table 3 reports the average score over all  $200 \times 2$  or  $250 \times 2$  samples for each mutation. Since a zero score indicates that a mutated image fails to satisfy one requirement, we deem scores within  $[0, 1)$  as failing and mark them in red. We view scores larger than two as satisfying the requirement. Specifically, scores within  $(2, 4]$  are marked in blue, whereas scores within  $(4, 5]$  are marked in green to highlight the best method for one mutation.

Fig. 3 shows mutation examples of different methods. Below, we interpret our human study results with these examples.

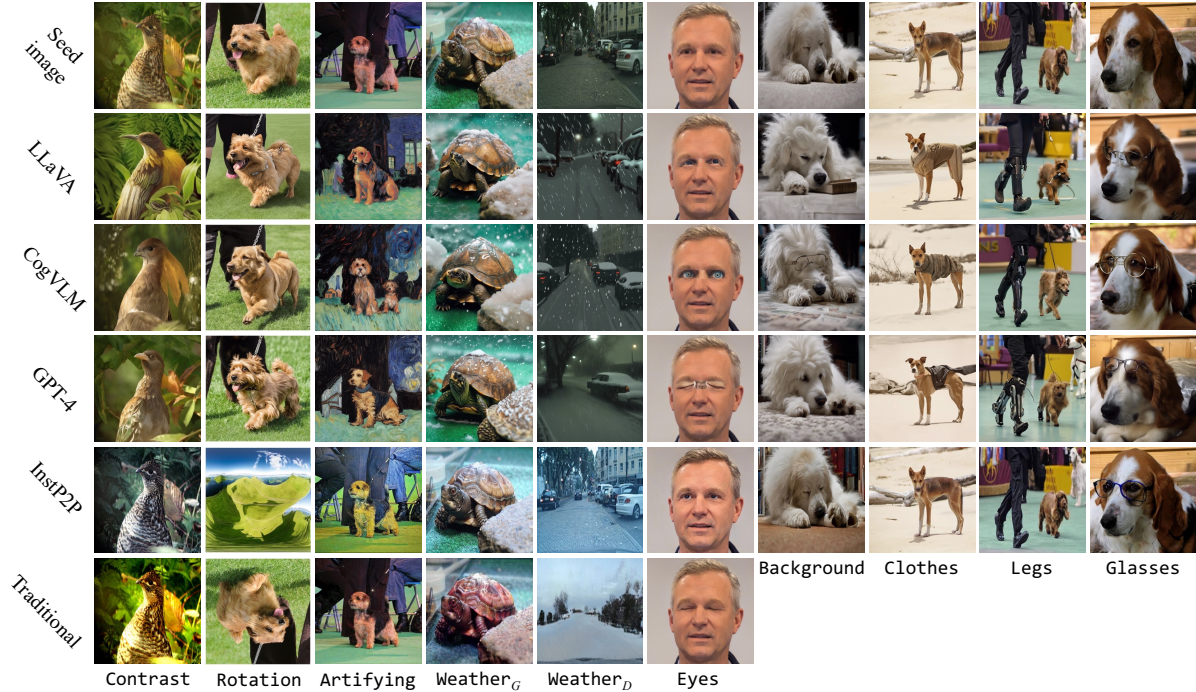


Figure 3: Mutation examples achieved via traditional method and different MLLMs.

**Contrast and Rotation:** Our results show that MLLMs are unable to implement pixel- and geometrical-level mutations, as supported by the red scores under the alignment evaluation. Note that pixel- and geometrical-level mutations directly operate on image pixels, whereas the remaining mutations focus on image features (i.e., image representations obtained using neural networks). MLLMs also primarily accept image features, leaving lower-level image semantics untouched. This explains why MLLMs fail in implementing pixel- and geometrical-level mutations, as images before and after these mutations often do not lead to notable changes in image features. Recent MLLM papers have similar observations: MLLMs perform worse in the spatial reasoning of image contents [7, 12, 49].

Different from others, InstP2P fails in the validity evaluation of *Rotation* and the faithfulness evaluation also has an average score of one. As shown in Fig. 3, InstP2P generates a meaningless image when implementing *Rotation*, and we find that similar failures occur in all evaluated samples. Recall as noted in Sec. 5.2, InstP2P differs from other MLLMs by its unidirectional pipeline: to complement the missing details in the text instruction, InstP2P fine-tunes the image generator (i.e., the Diffusion model) with mutation samples. We therefore suspect that the fine-tuning harms the generative capability of the Diffusion model. Hence, when implementing geometrical-level mutations that require spatial reasoning, InstP2P fails to generate valid images. In contrast, as other MLLMs do not modify the image generator, they mostly “transmit” the seed images if they cannot implement a mutation.

**Artifying:** MLLMs outperform traditional methods in transferring the artistic style of images. Past methods often extract the artistic style from one or a few target images, whose understanding of the target style may be limited. Moreover, traditional style transfer may fail if contents in the seed image and the target have distinct geometrical structures. These two limitations explain why the alignment score of traditional method is unsatisfactory (i.e., only 1.7). MLLMs encode general knowledge and can better comprehend the target style from their immense amounts of training data.

However, MLLM’s faithfulness results are relatively worse than those of traditional methods. As shown in Fig. 3, besides transferring the style, MLLMs also edit other irrelevant semantics in the mutated images. This observation is consistent with our findings mentioned above: MLLMs often focus on high-level features and neglect low-level details. As a result, such details are lost and consequently “inpainted” with random ones when generating mutated images.

**Snow<sub>G</sub> and Snow<sub>D</sub>:** InstP2P fails to transfer weather conditions for general images and driving scenes. We attribute the reason to the lack of fine-tuning data. To support transferring weather conditions, the fine-tuning in InstP2P requires mutation variants of the seed image that contain different weather conditions, and such data tuples are hard to prepare in large scale. Thus, the fine-tuned Diffusion model in InstP2P is unable to capture the weather conditions, transmitting the input image to the output in most cases, as indicated by the high faithfulness and validity score. The traditional method leverages the cycle-consistency to achieve weather transfer without requiring paired images as the guidance. This paradigm suc-

cessfully transfers the weather conditions for diving scenes, resulting in a high alignment score. However, it fails to retain the faithfulness (i.e., a 0.2 score), such that mutated images do not preserve irrelevant semantics, as presented in Fig. 3. In addition, the cycle-consistency relies on the similar geometrical structure between the seed and target images; this explains why traditional method is inapplicable to mutate weather conditions in general images whose geometrical structures are largely distinct from driving scenes.

The other three MLLMs, especially GPT-4V, have satisfactory alignment, faithfulness, and validity when transferring weather conditions for both general images and driving scenes. We attribute these to the general knowledge encoded in MLLMs. Although fine-grained details are also modified in MLLM’s generated images (see Fig. 3), we envision MLLM’s promising application in testing VDL systems where weather conditions are crucial (e.g., auto-driving).

**Eyes:** Traditional methods outperform MLLMs when implementing perceptual-level mutations. All MLLMs are unable to deliver satisfactory alignment scores. As in Fig. 3, all MLLMs do not close the eyes but replace them with new eyes in most cases. That is, these MLLMs understand that the mutation modifying eyes but cannot precisely mutate eyes. Moreover, recall that as mentioned in Sec. 3, the traditional implementation of *Eyes* requires specifying the localization of eyes. To make the comparison fair, we also provide the eye locations to MLLMs. However, as shown in Fig. 3, MLLMs fail to generate smoothly mutated images and the edited eyes look unnatural, leading to relatively lower validity scores.

**MLLM-Enabled (⑦-⑩):** Our results show that only InstP2P can implement *Background* to a satisfactory level, whereas the other three MLLMs tend to not edit the seed image in *Background*, as indicated by the relatively high faithfulness and validity score (see examples in Fig. 3). However, the trend is on the opposite when implementing *Clothes* and *Legs*, where InstP2P has lower alignment scores but much higher faithfulness and validity scores. For *Glasses*, all MLLMs have satisfactory alignment, faithfulness, and validity scores, and InstP2P outperforms the other three MLLMs.

To understand these distinct results, we need to dig into the key difference between mutations ⑦-⑩. Holistically, *Glasses* and *Background* are more “silent” whereas *Clothes* and *Legs* are more “active”. *Background* focuses on the background, whereas the other three mutations edit the subjects in the seed image. *Glasses* can be viewed as the simplest form of semantic-additive mutation as it is similar to “inserting” a new object into the seed; it only requires locating the eyes and putting the glasses on without altering other content. *Clothes* and *Legs*, in contrast, require additionally modifying the remaining semantics for coherence consideration.

## 7 Quantitative Evaluation

We also conduct a large-scale quantitative evaluation to assess these input mutations using popular numerical metrics. While

the human study results are sufficient to reflect the quality of MLLM-produced test inputs, we wish the quantitative evaluations, which are automated and larger-scale, can further justify the human study results and provide insights from different angles.

### 7.1 Alignment and Faithfulness Evaluation

Our evaluated mutations focus on different semantics and operate at distinct levels. Thus, the alignment and faithfulness evaluations rely on the implementation of a mutation. We separately design alignment and faithfulness evaluations for different mutations.

Table 4: Evaluation results of Contrast & Rotation.

	Contrast: MSE	Rotation: SSIM
LLaVA	3039.72	0.177
CogVLM	3112.78	0.178
GPT-4V	3034.89	0.175
InstP2P	2532.89	0.134

**Contrast (①) and Rotation (②):** Given that pixel- and geometrical-level mutations are explicitly defined as mathematical transformations, mutations implemented using traditional methods are the ground truth. Also, considering that these two types of mutations globally mutate all pixels, it is infeasible to separately evaluate the alignment and faithfulness using numerical metrics. Therefore, we jointly evaluate the alignment and faithfulness of *Contrast* and *Rotation* implemented using MLLMs by comparing their mutated images with those of traditional methods. Specifically, because *Contrast* uniformly edits all pixel values, we compute the Mean Squared Error (MSE) between pixel values of images produced by MLLMs and traditional methods. A lower MSE value indicates that the MLLM-produced images are closer to the ground truth. For *Rotation*, since it moves the locations of pixels, we use SSIM, a metric of image structure-wise similarity, to quantify the differences between images mutated by MLLMs and traditional methods. The SSIM value ranges within  $[0, 1]$  and a higher value indicates that the MLLM’s mutated image is more similar to the ground truth.

Results are in Table 4. For *Contrast*, the differences between MLLM’s mutation and the ground truth are high. As a reference, the average MSE between seed images and their mutated outputs using *Contrast* is 1167.16, showing that MLLM’s mutated images largely deviate from the expected mutation. The MSE of InstP2P is lower than other three MLLMs, which is aligned to our human study results, where InstP2P’s alignment score is 1.2 and other MLLMs’ alignment scores are  $< 1$ . *Rotation* implemented using MLLMs are largely dissimilar to the ground truth (higher SSIM values denoting better results). The SSIM value of InstP2P is much lower than other MLLMs. This is aligned to our human study results: InstP2P generates invalid images under *Rotation* and results in much lower faithfulness and validity scores.

Hence, we conclude that MLLMs can hardly support pixel- and geometrical-level mutations.

Table 5: Quantitative results of style-level mutations.

		Artifying	Snow <sub>G</sub>	Snow <sub>D</sub>
Style loss* (Alignment)	LLaVA	2.67	1.94	1.06
	CogVLM	2.73	1.93	1.08
	GPT-4V	2.62	2.12	1.13
	InstP2P	2.60	1.70	1.03
	Traditional	2.39	1.23	1.06
Content loss (Faithfulness)	LLaVA	8.96	8.21	4.18
	CogVLM	8.90	8.01	3.90
	GPT-4V	8.25	7.98	4.12
	InstP2P	<b>4.92</b>	<b>2.43</b>	<b>1.03</b>
	Traditional	<b>3.02</b>	<b>2.97</b>	3.74

\* The unit of style loss is 1e-4.

**Style-level Mutations** (③-⑤). Recall that as mentioned in Sec. 3.2, style-level mutations separate an image as the content and style and aim to edit the image’s style. Therefore, following existing works on style-level mutations, we evaluate the alignment and faithfulness of style-level mutations with the style loss  $L_{\text{style}}$  and content loss  $L_{\text{content}}$  [23], respectively. The  $L_{\text{style}}$  prepares a set of images having the target “style” (e.g., Van Gogh’s paintings, or photos taken on snowy days) and extracts their style features using a pre-trained feature extractor. It then extracts the style feature from the mutated image and compares it with the target style features. A lower  $L_{\text{style}}$  value indicates a better alignment. Similarly, the  $L_{\text{content}}$  extracts and compares the content features of the seed image and the mutated image; a lower  $L_{\text{content}}$  value indicates a better faithfulness.

As shown in Table 5, although the style loss is widely used in existing style-level mutation works for benchmark or optimization, it cannot notably distinguish results of different implementations and is unable to reveal our findings in the human studies. The content loss, in contrast, varies among different implementations of the same style-level mutation. For Artifying and Snow<sub>G</sub>, the content loss values of InstP2P and traditional method are largely lower than others. Similarly, Snow<sub>D</sub> implemented using InstP2P also has a much lower content loss, indicating the content of the seed image is mostly preserved in the mutated image. These results are consistent to the faithfulness evaluations in our human studies. Overall, InstP2P tends to *not* mutate the seed image when implementing all style-level mutations. Traditional methods hardly mutate the weather conditions of general images (Snow<sub>G</sub>) and only slightly apply artistic style to seed images (Artifying).

**MLLM-enabled Mutations** (⑦-⑩): Due to the lack of ground truth and reference images for mutations ⑦-⑩, we evaluate their alignment via CLIP [48] following recent MLLM papers [28, 53, 68]. The CLIP can obtain unified embeddings for image semantics and text descriptions, enabling their similarity measurement. We first prepare the textual description of the anticipated mutation result for each mutation,

Table 6: Anticipated results of MLLM-enabled mutations.

Mutation	Textual description of mutation results
Background	“The background of this image is a library.”
Clothes	“A dog wearing clothes.”
Legs	“A dog with bionic legs.”
Glasses	“A dog with glasses.”

as shown in Table 6. For example, when mutating a dog image with Glasses, the mutated image should have “a dog with glasses”. We then use the CLIP to extract the embedding vectors for the mutated image and its corresponding textual description in Table 6; their cosine similarity is adopted to quantify the alignment of the mutation.

The faithfulness evaluation requires separating the local and fine-grained semantics such as eyes and legs from the image, which is challenging especially when the locations and postures of the dog are diverse. Therefore, we design a coarse-grained metric that only considers an image’s background and subject. Specifically, following [31], we employ the SoTA subject extractor InSPyReNet [38] to separate the subjects and background for the seed and mutated images. For Background, we use the similarity of the two subjects in the seed and mutated image as the faithfulness result, whereas for ⑧-⑩, we instead use the similarity of two backgrounds. Since semantic-additive mutations may alter the subject’s outline (e.g., adding clothes may change the dog’s shape), we compute the similarity as the cosine similarity between CLIP image embeddings of the extracted subjects/backgrounds.

Table 7: Alignment (left) and faithfulness (right) results of MLLM-enabled mutations.

	Background		Clothes		Legs		Glasses	
LLaVA	0.67	0.96	0.49	0.97	0.43	0.97	0.50	0.96
CogVLM	0.67	0.96	0.49	0.97	0.43	0.96	0.50	0.96
GPT-4V	0.67	0.96	0.49	0.97	0.43	0.97	0.50	0.97
InstP2P	0.69	0.95	0.50	0.97	0.44	0.97	0.52	0.97

Table 7 presents the results of alignment and faithfulness evaluations for four MLLM-enabled mutations. Different from our human studies, the two numerical metrics cannot distinguish the alignment and faithfulness of different MLLMs, despite that they are widely adopted to benchmark MLLMs [28, 53, 68]. The cosine similarity values in Table 7 range from -1 to 1, and the CLIP embedding often cannot capture relations between objects in the text [63, 70]. In that sense, the moderately high alignment results (all are positive and are greater than 0.4) in Table 7 indicate that these “semantic-additive” mutations do generate the new semantics. However, since MLLMs have varying capabilities to comprehend relations among objects, they may put the added semantics into a wrong position. For example, as in Fig. 3, when implementing Legs, GPT-4V makes the person’s legs bionic rather than the dog, which can be identified by humans and results in lower

alignment scores in Table 3. All MLLMs have almost perfect faithfulness results in Table 7, indicating that MLLMs are capable of limiting their implemented mutations within the mutated subjects or background semantics.

Table 8: Faithfulness results of Eyes.

	LLaVA	CogVLM	GPT-4V	InstP2P	Traditional
MSE	<b>17.97</b>	85.27	<b>18.03</b>	1014.97	200.79

**Perceptual-level Mutation (©).** Perceptual-level mutations also lack ground truth and reference images. Although the anticipated mutation result of Eyes can be described as “a person with closed eyes”, we find that the CLIP embeddings mentioned above cannot capture such detailed eye status in both text and image. Therefore, we only evaluate the faithfulness for Eyes. Because eyes in FFHQ dataset locate in a unified region, we can easily mask out the eyes and check if the remaining pixels are modified. The pixel difference is calculated using MSE; a lower value indicates a better faithfulness.

Interestingly, Table 8 seemingly contradicts our human study results: the MSE of LLaVA and GPT-4V are much lower than traditional method, whereas human participants rate traditional method as the best in the faithfulness evaluation. Consider the mutation examples in Fig. 3, LLaVA- and GPT-4V-implemented mutations indeed replace eyes in the seed image, which limits the mutated region within the eyes but produces unnatural images. Such unnaturalness negatively impacts the faithfulness under human’s view. In contrast, the traditional method slightly edits other relevant semantics (e.g., muscles around the eyes) to generate naturally mutated images. Despite that pixels outside the eyes are also modified, these changed pixels are unaware under human observation.

## 7.2 Validity Evaluation

Since MLLMs cannot implement pixel-, geometrical-, and perceptual-level mutations as evaluated in Sec. 6.2 and Sec. 7.1, we use numerical metrics to evaluate the validity for style-level (③-⑤) and MLLM-enabled mutations (⑦-⑩).

Table 9: Validity results of style-level mutations.

	IS	FID	Precision	Recall
LLaVA	18.26	120.49	0.33	0.29
CogVLM	17.11	124.30	0.34	0.34
GPT-4V	17.61	123.70	0.39	0.31
InstP2P	20.17	127.95	0.35	0.24
Traditional	19.84	124.51	0.46	0.19

**IS and FID Metrics.** Following existing works, we take two popular metrics, Inception Score (IS) [51] and Fréchet Inception Distance (FID) [29], to measure the validity of the mutated images. Both IS and FID use a set of real images as the reference, and compare the mutated images with these

Table 10: Validity results of MLLM-enabled mutations.

	IS	FID	Precision	Recall
LLaVA	14.51	88.09	0.58	0.33
CogVLM	13.71	89.65	0.60	0.34
GPT-4V	14.82	88.67	0.53	0.36
InstP2P	23.93	93.95	0.58	0.35

reference images to estimate how likely the mutated images are real. A lower FID value indicates a better realism, whereas a higher IS value indicates a better realism.

**Precision & Recall.** Although IS/FID are widely used by image generation and VDL testing to assess how realistic an image is [26, 65], they jointly consider the validity and diversity. Some of our evaluated mutations are non-deterministic (e.g., style-level mutations), where multiple (possible) mutated images can be produced using one seed image. Thus, a better IS or FID result may be due to diversified mutations, not a better validity. We use the Precision & Recall metrics [39, 50] to separately evaluate the validity and diversity, respectively. The Precision & Recall here are different from the conventional precision/recall that count positive and negative results; they are new metrics proposed to assess image quality. Both Precision & Recall range within [0, 1] and higher is better.

Table 9 shows results of the validity evaluation for style-level mutations implemented using traditional methods and different MLLMs. Considering the high magnitude of FID values, both IS and FID results cannot notably distinguish different methods. When separately evaluating the validity and diversity, traditional method has the highest validity (Precision) but the lowest diversity (Recall). That is, MLLMs are superior in diversifying the seed images with style-level mutations, whereas traditional method can better preserve the validity.

Validity results of MLLM-enabled mutations are given in Table 10. Only IS values can distinguish different MLLMs and InstP2P has the best IS result, which is consistent with our human study results where InstP2P largely outperforms other MLLMs in the validity evaluation of Clothes and Legs. By cross-comparing results in Table 10 and Table 9, especially FID, Precision, and Recall values, we can see that MLLMs perform better on the semantic-additive mutations than on the style-level mutations, as supported by both better validity and diversity (note that lower FID is better).

## 7.3 Testing Effectiveness Evaluation

We also employ mutated images generated from different mutations to test VDL models and evaluate their effectiveness in triggering VDL faults. Given the wide adoption of VDL systems, it is impractical to consider all VDL applications. We therefore choose different VDL-based classifiers as one representative application.

Table 11: Testing effectiveness of different mutations, i.e., averaged ( $\#VDL$  faults)/( $\#test$  inputs).

VDL Model		Contrast	Rotation	Artiflying	Snow <sub>G</sub>	Background	Clothes	Legs	Glasses
ConvNeXt	LLaVA	N/A	N/A	7.6%	4.8%	5.2%	7.7%	2.8%	7.7%
	CogVLM			9.6%	4.8%	7.6%	10.1%	4.5%	8.6%
	GPT-4V			9.2%	3.6%	6.8%	9.7%	1.6%	5.7%
	InstP2P			6.4%	4.4%	11.2%	1.2%	1.2%	0.8%
	Traditional			6.0%	0.4%	6.8%	14.4%	N/A	
<b>Avg.</b>	6.0%	0.4%	7.9%	6.4%	7.7%	7.2%	2.5%	5.7%	
SwinTransformer	LLaVA	N/A	N/A	8.0%	4.8%	5.2%	7.3%	2.8%	7.7%
	CogVLM			9.6%	4.8%	7.2%	10.9%	4.5%	9.4%
	GPT-4V			9.2%	4.4%	7.2%	9.3%	1.6%	6.1%
	InstP2P			5.6%	4.0%	13.2%	2.8%	1.6%	2.0%
	Traditional			6.8%	0.4%	8.4%	16.0%	N/A	
<b>Avg.</b>	6.8%	0.4%	8.2%	6.8%	8.2%	7.6%	2.6%	6.3%	
ViT	LLaVA	N/A	N/A	8.0%	4.8%	4.4%	7.7%	3.2%	6.1%
	CogVLM			9.6%	5.2%	7.6%	10.5%	4.9%	9.8%
	GPT-4V			7.6%	4.4%	7.6%	10.1%	0.8%	5.3%
	InstP2P			7.2%	3.6%	12.0%	2.0%	1.6%	1.6%
	Traditional			8.4%	0.4%	7.2%	16.0%	N/A	
<b>Avg.</b>	8.4%	0.4%	7.9%	6.8%	7.9%	7.6%	2.6%	5.7%	

We choose three recent SoTA VDL-based classifiers, Vision Transformer (ViT) [17], SwinTransformer (SwinT) [44], and ConvNeXt [45]. These models are officially released by PyTorch and are trained with ImageNet, where Snow<sub>D</sub> (⑤) and Eyes (⑥) are inapplicable. Mutated images are fed into a popular VDL testing tool DeepHunter [62] to detect VDL faults. DeepHunter implements a checker to rule out potentially broken, invalid mutated images to reduce false positive VDL faults. We configure its checker such that invalid images can be mostly filtered out, per our observation.

Results are given in Table 11. While the same seed images are used, images generated using different mutations have distinct effectiveness when triggering VDL faults. Pixel-level (①) and style-level mutation (③ and ④) have high effectiveness on average. This is consistent with the texture bias revealed in [24]: modern image classifiers are sensitive to perturbations of texture in images. Here, texture refers to the appearance of an object’s surface, such as the intensity and the arrangement of colors. Both pixel- and style-level mutations modify texture-related semantics and can more frequently trigger VDL faults.

Interestingly, while Snow<sub>G</sub> (④) implemented using traditional method mostly does not mutate the seed image (see Sec. 6.2 and Sec. 7.1), their unperceivable perturbations can effectively mislead the tested VDL model. Despite the high effectiveness, considering that Snow<sub>G</sub> is not accurately implemented, these mutated images should be less valuable as they give a false sense that the tested VDL model is sensitive to weather conditions. For the four MLLM-enabled mutations (⑦-⑩), Background (⑦) and Clothes (⑧) have the highest effectiveness. Given that Background does not alter the subject based on our results in Sec. 6.2 and Sec. 7.1, we suspect that these SoTA VDL models may largely rely

on background semantics to recognize the subject. Clothes often generates unusual combinations of semantics, e.g., a dog wearing clothes may less likely to appear in these models’ training data. Thus, it is reasonable that Clothes is more effective to challenge the tested VDL models. Legs (⑨) and Glasses (⑩) are less effective because their mutated semantics (i.e., legs and eyes) are not crucial to recognize dogs.

## 8 Lessons, Discussion, and Threat To Validity

This paper aims to understand the status quo of MLLM-based VDL testing and provide insights. We also explicate the further efforts required to link MLLMs with VDL testing. Our study enhances the confidence in using MLLMs (and in general, LLMs) within the testing community. While to date, one can expect an “out-of-the-box” usage of MLLMs for testing VDL systems under some real-world scenarios, we present the following lessons and discussions.

**New Mutations.** Our evaluation shows that MLLMs are suitable for mutations *transferring semantics* between images, e.g., style-level mutations that transfer styles, and semantic-additive mutations that add new semantics (from other images) to the seed. These are highly valuable in VDL testing, as they can generate diverse and valid test inputs, and importantly, these mutations are hardly feasible with traditional methods. We thus believe it is high time to incorporate MLLMs into VDL testing tasks, which shall enable comprehensive and finer-grained testing of VDL systems where subtle semantic changes are critical and can lead to catastrophic failures, such as in autonomous driving and drone navigation. Nevertheless, contemporary MLLMs are less capable of *editing existing semantics*. That said, despite the optimism, MLLMs are not a panacea for all VDL testing tasks. We thus advocate to inte-

grate and carefully choose MLLMs and traditional methods in VDL testing.

**Different MLLM Pipelines.** By comparing MLLM pipelines (as introduced in Sec. 5.2) and considering semantic-additive mutations, the unidirectional and fine-tuning-based pipeline appears more applicable to silent mutations that modify the image background or subtly alter the image subject. The bidirectional pipeline is superior in actively editing the subject. These findings suggest that different MLLM pipelines have distinct capabilities in reasoning the relations among objects, leading to varied performance for different mutations. Therefore, we suggest users choose the MLLM pipeline based on the mutation’s extent and the testing target (e.g., a VDL’s robustness to varied backgrounds or subjects). Moreover, this finding highlights the importance of understanding and decomposing scenes in seed images before mutating subjects or backgrounds; emerging research sheds light on this direction [54, 69].

**Threat to Validity.** The human study may be biased, and to mitigate this threat, we have involved 20 participants with relevant expertise. We presume that it is sufficient to guarantee the credibility of our study. We also conducted a quantitative evaluation to complement the human study. Second, the numerical criteria used in the quantitative evaluation may not fully capture the quality of the generated images. To mitigate this, we follow the existing criteria (e.g., FID and IS) used in the literature. Moreover, our findings may not be generalizable; we mitigate this by using diverse sets of images, mutation methods, MLLMs, and VDL systems.

## 9 Conclusion

This paper presents an in-depth study on MLLM-produced test inputs for VDL testing. We categorize image mutation methods and evaluate their quality using several criteria. We provide insights into the (in-)adequacy of MLLMs for VDL testing and advocate for the careful integration of MLLMs and traditional image mutation methods for better testing effectiveness and application scenarios.

## References

- [1] Amazon mechanical turk. <https://www.mturk.com/>.
- [2] Kaggle competition: Dog breed identification. <https://www.kaggle.com/competitions/dog-breed-identification>.
- [3] Dalle. <https://openai.com/dall-e-2>, 2023.
- [4] Stable diffusion online. <https://github.com/CompVis/stable-diffusion>, 2023.
- [5] Josh Achiam, Steven Adler, Sandhini Agarwal, Lama Ahmad, Ilge Akkaya, Florencia Leoni Aleman, Diogo Almeida, Janko Altschmidt, Sam Altman, Shyamal Anadkat, et al. GPT-4 technical report. *arXiv preprint arXiv:2303.08774*, 2023.
- [6] Jacob Austin, Augustus Odena, Maxwell I. Nye, Maarten Bosma, Henryk Michalewski, David Dohan, Ellen Jiang, Carrie J. Cai, Michael Terry, Quoc V. Le, and Charles Sutton. Program synthesis with large language models. 2021.
- [7] Yejin Bang, Samuel Cahyawijaya, Nayeon Lee, Wenhao Dai, Dan Su, Bryan Wilie, Holy Lovenia, Ziwei Ji, Tiezheng Yu, Willy Chung, Quyet V. Do, Yan Xu, and Pascale Fung. A multitask, multilingual, multimodal evaluation of ChatGPT on reasoning, hallucination, and interactivity. In Jong C. Park, Yuki Arase, Baotian Hu, Wei Lu, Derry Wijaya, Ayu Purwarianti, and Adila Alfa Krisnadhi, editors, *Proceedings of the 13th International Joint Conference on Natural Language Processing and the 3rd Conference of the Asia-Pacific Chapter of the Association for Computational Linguistics (Volume 1: Long Papers)*, pages 675–718, Nusa Dua, Bali, November 2023. Association for Computational Linguistics.
- [8] Tim Brooks, Aleksander Holynski, and Alexei A Efros. Instructpix2pix: Learning to follow image editing instructions. In *Proceedings of the IEEE/CVF Conference on Computer Vision and Pattern Recognition*, pages 18392–18402, 2023.
- [9] Davide Caffagni, Federico Cocchi, Luca Barsellotti, Nicholas Moratelli, Sara Sarto, Lorenzo Baraldi, Marcella Cornia, and Rita Cucchiara. The (r) evolution of multimodal large language models: A survey. *arXiv preprint arXiv:2402.12451*, 2024.
- [10] Hila Chefer, Yuval Alaluf, Yael Vinker, Lior Wolf, and Daniel Cohen-Or. Attend-and-excite: Attention-based semantic guidance for text-to-image diffusion models. *ACM Transactions on Graphics (TOG)*, 42(4):1–10, 2023.
- [11] Wei-Ge Chen, Irina Spiridonova, Jianwei Yang, Jianfeng Gao, and Chunyuan Li. Llava-interactive: An all-in-one demo for image chat, segmentation, generation and editing. *arXiv preprint arXiv:2311.00571*, 2023.
- [12] Anthony G Cohn and Jose Hernandez-Orallo. Dialectical language model evaluation: An initial appraisal of the commonsense spatial reasoning abilities of llms. *arXiv preprint arXiv:2304.11164*, 2023.
- [13] Marius Cordts, Mohamed Omran, Sebastian Ramos, Timo Rehfeld, Markus Enzweiler, Rodrigo Benenson, Uwe Franke, Stefan Roth, and Bernt Schiele. The cityscapes dataset for semantic urban scene understanding. In *Proceedings of the IEEE conference on computer vision and pattern recognition*, pages 3213–3223, 2016.
- [14] Jia Deng, Wei Dong, Richard Socher, Li-Jia Li, Kai Li, and Li Fei-Fei. Imagenet: A large-scale hierarchical image database. In *2009 IEEE conference on computer vision and pattern recognition*, pages 248–255. IEEE, 2009.
- [15] Yinlin Deng, Chunqiu Steven Xia, Haoran Peng, Chenyuan Yang, and Lingming Zhang. Large language models are zero-shot fuzzers: Fuzzing deep-learning libraries via large language models. In *Proceedings of*

- the 32nd ACM SIGSOFT international symposium on software testing and analysis*, pages 423–435, 2023.
- [16] Swaroopa Dola, Matthew B Dwyer, and Mary Lou Soffa. Distribution-aware testing of neural networks using generative models. In *2021 IEEE/ACM 43rd International Conference on Software Engineering (ICSE)*, pages 226–237. IEEE, 2021.
- [17] Alexey Dosovitskiy, Lucas Beyer, Alexander Kolesnikov, Dirk Weissenborn, Xiaohua Zhai, Thomas Unterthiner, Mostafa Dehghani, Matthias Minderer, Georg Heigold, Sylvain Gelly, Jakob Uszkoreit, and Neil Houlsby. An image is worth 16x16 words: Transformers for image recognition at scale. In *International Conference on Learning Representations*, 2021.
- [18] Chengbin Du, Yanxi Li, Zhongwei Qiu, and Chang Xu. Stable diffusion is unstable. *Advances in Neural Information Processing Systems*, 36, 2024.
- [19] Isaac Dunn, Hadrien Pouget, Daniel Kroening, and Tom Melham. Exposing previously undetectable faults in deep neural networks. In *Proceedings of the 30th ACM SIGSOFT International Symposium on Software Testing and Analysis*, pages 56–66, 2021.
- [20] Zhiyu Fan, Xiang Gao, Martin Mirchev, Abhik Roychoudhury, and Shin Hwei Tan. Automated repair of programs from large language models. In *2023 IEEE/ACM 45th International Conference on Software Engineering (ICSE)*, pages 1469–1481. IEEE, 2023.
- [21] Weixi Feng, Xuehai He, Tsu-Jui Fu, Varun Jampani, Arjun Reddy Akula, Pradyumna Narayana, Sugato Basu, Xin Eric Wang, and William Yang Wang. Training-free structured diffusion guidance for compositional text-to-image synthesis. In *The Eleventh International Conference on Learning Representations*, 2023.
- [22] Tsu-Jui Fu, Wenze Hu, Xianzhi Du, William Yang Wang, Yinfei Yang, and Zhe Gan. Guiding Instruction-based Image Editing via Multimodal Large Language Models. In *International Conference on Learning Representations (ICLR)*, 2024.
- [23] Leon A Gatys, Alexander S Ecker, and Matthias Bethge. Image style transfer using convolutional neural networks. In *Proceedings of the IEEE conference on computer vision and pattern recognition*, pages 2414–2423, 2016.
- [24] Robert Geirhos, Patricia Rubisch, Claudio Michaelis, Matthias Bethge, Felix A Wichmann, and Wieland Brendel. Imagenet-trained cnns are biased towards texture; increasing shape bias improves accuracy and robustness. In *International Conference on Learning Representations*, 2018.
- [25] Ian J Goodfellow, Jonathon Shlens, and Christian Szegedy. Explaining and harnessing adversarial examples. In *International Conference on Learning Representations*, 2015.
- [26] Fabrice Harel-Canada, Lingxiao Wang, Muhammad Ali Gulzar, Quanquan Gu, and Miryung Kim. Is neuron coverage a meaningful measure for testing deep neural networks? In *Proceedings of the 28th ACM Joint Meeting on European Software Engineering Conference and Symposium on the Foundations of Software Engineering*, pages 851–862, 2020.
- [27] Erik Härkönen, Aaron Hertzmann, Jaakko Lehtinen, and Sylvain Paris. Ganspace: Discovering interpretable gan controls. *Advances in neural information processing systems*, 33:9841–9850, 2020.
- [28] Amir Hertz, Ron Mokady, Jay Tenenbaum, Kfir Aberman, Yael Pritch, and Daniel Cohen-Or. Prompt-to-prompt image editing with cross attention control. *arXiv preprint arXiv:2208.01626*, 2022.
- [29] Martin Heusel, Hubert Ramsauer, Thomas Unterthiner, Bernhard Nessler, and Sepp Hochreiter. Gans trained by a two time-scale update rule converge to a local nash equilibrium. In *Advances in neural information processing systems*, pages 6626–6637, 2017.
- [30] Jonathan Ho, Ajay Jain, and Pieter Abbeel. Denoising diffusion probabilistic models. *Advances in neural information processing systems*, 33:6840–6851, 2020.
- [31] Miao Hua, Jiawei Liu, Fei Ding, Wei Liu, Jie Wu, and Qian He. Dreamtuner: Single image is enough for subject-driven generation. *arXiv preprint arXiv:2312.13691*, 2023.
- [32] Yi Huang, Jiancheng Huang, Yifan Liu, Mingfu Yan, Jiaxi Lv, Jianzhuang Liu, Wei Xiong, He Zhang, Shifeng Chen, and Liangliang Cao. Diffusion model-based image editing: A survey. *arXiv preprint arXiv:2402.17525*, 2024.
- [33] Yuzhou Huang, Liangbin Xie, Xintao Wang, Ziyang Yuan, Xiaodong Cun, Yixiao Ge, Jiantao Zhou, Chao Dong, Rui Huang, Ruimao Zhang, et al. Smartedit: Exploring complex instruction-based image editing with multimodal large language models. *arXiv preprint arXiv:2312.06739*, 2023.
- [34] Naman Jain, Skanda Vaidyanath, Arun Shankar Iyer, Nagarajan Natarajan, Suresh Parthasarathy, Sriram K. Rajamani, and Rahul Sharma. Jigsaw: Large language models meet program synthesis. In *Proc. ACM ICSE*, 2022.
- [35] Sungmin Kang, Robert Feldt, and Shin Yoo. Sinvad: Search-based image space navigation for dnn image classifier test input generation. In *Proceedings of the IEEE/ACM 42nd International Conference on Software Engineering Workshops*, pages 521–528, 2020.
- [36] Tero Karras, Samuli Laine, and Timo Aila. A style-based generator architecture for generative adversarial networks. In *Proceedings of the IEEE/CVF conference on computer vision and pattern recognition*, pages 4401–4410, 2019.
- [37] Hyunsu Kim, Yunjey Choi, Junho Kim, Sungjoo Yoo,

- and Youngjung Uh. Exploiting spatial dimensions of latent in gan for real-time image editing. In *Proceedings of the IEEE/CVF Conference on Computer Vision and Pattern Recognition*, pages 852–861, 2021.
- [38] Taehun Kim, Kunhee Kim, Joonyeong Lee, Dongmin Cha, Jiho Lee, and Daijin Kim. Revisiting image pyramid structure for high resolution salient object detection. In *Proceedings of the Asian Conference on Computer Vision*, pages 108–124, 2022.
- [39] Tuomas Kynkäänniemi, Tero Karras, Samuli Laine, Jaakko Lehtinen, and Timo Aila. Improved precision and recall metric for assessing generative models. *Advances in neural information processing systems*, 32, 2019.
- [40] John A Lee and Michel Verleysen. *Nonlinear dimensionality reduction*. Springer Science & Business Media, 2007.
- [41] Bohao Li, Yuying Ge, Yixiao Ge, Guangzhi Wang, Rui Wang, Ruimao Zhang, and Ying Shan. Seed-bench-2: Benchmarking multimodal large language models. *arXiv preprint arXiv:2311.17092*, 2023.
- [42] Huan Ling, Karsten Kreis, Daiqing Li, Seung Wook Kim, Antonio Torralba, and Sanja Fidler. Editgan: High-precision semantic image editing. *Advances in Neural Information Processing Systems*, 34:16331–16345, 2021.
- [43] Haotian Liu, Chunyuan Li, Qingyang Wu, and Yong Jae Lee. Visual instruction tuning. *Advances in neural information processing systems*, 36, 2024.
- [44] Ze Liu, Yutong Lin, Yue Cao, Han Hu, Yixuan Wei, Zheng Zhang, Stephen Lin, and Baining Guo. Swin transformer: Hierarchical vision transformer using shifted windows. In *Proceedings of the IEEE/CVF international conference on computer vision*, pages 10012–10022, 2021.
- [45] Zhuang Liu, Hanzi Mao, Chao-Yuan Wu, Christoph Feichtenhofer, Trevor Darrell, and Saining Xie. A convnet for the 2020s. In *Proceedings of the IEEE/CVF conference on computer vision and pattern recognition*, pages 11976–11986, 2022.
- [46] Kexin Pei, Yinzhi Cao, Junfeng Yang, and Suman Jana. DeepXplore: Automated whitebox testing of deep learning systems. In *Proceedings of the 26th Symposium on Operating Systems Principles, SOSP ’17*, pages 1–18, 2017.
- [47] Yun Peng, Shuzheng Gao, Cuiyun Gao, Yintong Huo, and Michael Lyu. Domain knowledge matters: Improving prompts with fix templates for repairing python type errors. In *Proceedings of the 46th IEEE/ACM International Conference on Software Engineering*, pages 1–13, 2024.
- [48] Alec Radford, Jong Wook Kim, Chris Hallacy, Aditya Ramesh, Gabriel Goh, Sandhini Agarwal, Girish Sastry, Amanda Askell, Pamela Mishkin, Jack Clark, et al. Learning transferable visual models from natural language supervision. In *International conference on machine learning*, pages 8748–8763. PMLR, 2021.
- [49] Yasaman Razeghi, Robert L Logan IV, Matt Gardner, and Sameer Singh. Impact of pretraining term frequencies on few-shot numerical reasoning. In Yoav Goldberg, Zornitsa Kozareva, and Yue Zhang, editors, *Findings of the Association for Computational Linguistics: EMNLP 2022*, pages 840–854, Abu Dhabi, United Arab Emirates, December 2022. Association for Computational Linguistics.
- [50] Mehdi SM Sajjadi, Olivier Bachem, Mario Lucic, Olivier Bousquet, and Sylvain Gelly. Assessing generative models via precision and recall. *Advances in Neural Information Processing Systems*, 31, 2018.
- [51] Tim Salimans, Ian Goodfellow, Wojciech Zaremba, Vicki Cheung, Alec Radford, and Xi Chen. Improved techniques for training gans. *Advances in neural information processing systems*, 29:2234–2242, 2016.
- [52] Yujun Shen, Jinjin Gu, Xiaoou Tang, and Bolei Zhou. Interpreting the latent space of gans for semantic face editing. In *Proceedings of the IEEE/CVF Conference on Computer Vision and Pattern Recognition*, pages 9243–9252, 2020.
- [53] Shelly Sheynin, Adam Polyak, Uriel Singer, Yuval Kirstain, Amit Zohar, Oron Ashual, Devi Parikh, and Yaniv Taigman. Emu edit: Precise image editing via recognition and generation tasks. *arXiv preprint arXiv:2311.10089*, 2023.
- [54] Mingzhen Sun, Weining Wang, Xinxin Zhu, and Jing Liu. Moso: Decomposing motion, scene and object for video prediction. In *Proceedings of the IEEE/CVF Conference on Computer Vision and Pattern Recognition*, pages 18727–18737, 2023.
- [55] Yuqiang Sun, Daoyuan Wu, Yue Xue, Han Liu, Haijun Wang, Zhengzi Xu, Xiaofei Xie, and Yang Liu. GPTScan: Detecting logic vulnerabilities in smart contracts by combining GPT with program analysis. In *Proc. ACM ICSE*, 2024.
- [56] Yuchi Tian, Kexin Pei, Suman Jana, and Baishakhi Ray. Deeptest: Automated testing of deep-neural-network-driven autonomous cars. In *Proceedings of the 40th international conference on software engineering*, pages 303–314, 2018.
- [57] Shuai Wang and Zhendong Su. Metamorphic object insertion for testing object detection systems. In *Proceedings of the 35th IEEE/ACM International Conference on Automated Software Engineering*, pages 1053–1065, 2020.
- [58] Weihang Wang, Qingsong Lv, Wenmeng Yu, Wenyi Hong, Ji Qi, Yan Wang, Junhui Ji, Zhuoyi Yang, Lei Zhao, Xixuan Song, et al. CogVLM: Visual expert for pretrained language models. *arXiv preprint arXiv:2311.03079*, 2023.

- [59] Cheng Wen, Jialun Cao, Jie Su, Zhiwu Xu, Shengchao Qin, Mengda He, Haokun Li, Shing-Chi Cheung, and Cong Tian. Enchanting program specification synthesis by large language models using static analysis and program verification. In *Proc. Springer CAV*, 2022.
- [60] Chunqiu Steven Xia, Matteo Paltenghi, Jia Le Tian, Michael Pradel, and Lingming Zhang. Universal fuzzing via large language models. *Proceedings of the 46th IEEE/ACM International Conference on Software Engineering*, 2024.
- [61] Chunqiu Steven Xia, Yuxiang Wei, and Lingming Zhang. Automated program repair in the era of large pre-trained language models. In *2023 IEEE/ACM 45th International Conference on Software Engineering (ICSE)*, pages 1482–1494. IEEE, 2023.
- [62] Xiaofei Xie, Lei Ma, Felix Juefei-Xu, Minhui Xue, Hongxu Chen, Yang Liu, Jianjun Zhao, Bo Li, Jianxiong Yin, and Simon See. Deephunter: a coverage-guided fuzz testing framework for deep neural networks. In *Proceedings of the 28th ACM SIGSOFT International Symposium on Software Testing and Analysis*, pages 146–157, 2019.
- [63] Lewei Yao, Runhui Huang, Lu Hou, Guansong Lu, Minzhe Niu, Hang Xu, Xiaodan Liang, Zhenguo Li, Xin Jiang, and Chunjing Xu. Filip: Fine-grained interactive language-image pre-training. In *International Conference on Learning Representations*, 2021.
- [64] Boxi Yu, Zhiqing Zhong, Xinran Qin, Jiayi Yao, Yuancheng Wang, and Pinjia He. Automated testing of image captioning systems. In *Proceedings of the 31st ACM SIGSOFT International Symposium on Software Testing and Analysis*, pages 467–479, 2022.
- [65] Yuanyuan Yuan, Qi Pang, and Shuai Wang. Provably valid and diverse mutations of real-world media data for dnn testing. *IEEE Transactions on Software Engineering*, 2024.
- [66] Yuanyuan Yuan, Shuai Wang, Mingyue Jiang, and Tsong Yueh Chen. Perception matters: Detecting perception failures of vqa models using metamorphic testing. In *Proceedings of the IEEE/CVF Conference on Computer Vision and Pattern Recognition*, pages 16908–16917, 2021.
- [67] Mengshi Zhang, Yuqun Zhang, Lingming Zhang, Cong Liu, and Sarfraz Khurshid. Deeproad: Gan-based metamorphic testing and input validation framework for autonomous driving systems. In *Proceedings of the 33rd ACM/IEEE International Conference on Automated Software Engineering*, pages 132–142, 2018.
- [68] Yuechen Zhang, Jinbo Xing, Eric Lo, and Jiaya Jia. Real-world image variation by aligning diffusion inversion chain. *Advances in Neural Information Processing Systems*, 36, 2024.
- [69] MI Zhenxing and Dan Xu. Switch-nerf: Learning scene decomposition with mixture of experts for large-scale neural radiance fields. In *The Eleventh International Conference on Learning Representations*, 2022.
- [70] Yiwu Zhong, Jianwei Yang, Pengchuan Zhang, Chunyuan Li, Noel Codella, Liunian Harold Li, Luwei Zhou, Xiyang Dai, Lu Yuan, Yin Li, et al. Regionclip: Region-based language-image pretraining. In *2022 IEEE/CVF Conference on Computer Vision and Pattern Recognition (CVPR)*, pages 16772–16782. IEEE Computer Society, 2022.
- [71] Jiapeng Zhu, Ruili Feng, Yujun Shen, Deli Zhao, Zheng-Jun Zha, Jingren Zhou, and Qifeng Chen. Low-rank subspaces in gans. *Advances in Neural Information Processing Systems*, 34:16648–16658, 2021.
- [72] Jiapeng Zhu, Yujun Shen, Deli Zhao, and Bolei Zhou. In-domain gan inversion for real image editing. In *European conference on computer vision*, pages 592–608. Springer, 2020.
- [73] Jun-Yan Zhu. CycleGAN Failure Cases. <http://github.com/junyanz/CycleGAN#failure-cases>, 2021.
- [74] Jun-Yan Zhu, Taesung Park, Phillip Isola, and Alexei A Efros. Unpaired image-to-image translation using cycle-consistent adversarial networks. In *Proceedings of the IEEE international conference on computer vision*, pages 2223–2232, 2017.